# EFFECTS OF CONSTRUCTION ON LATERALLY LOADED PILE GROUPS

By An-Bin Huang,[1] Chao-Kuang Hsueh,[2] Michael W. O'Neill,[3] S. Chern,[4] and C. Chen[5]

**ABSTRACT:** Full-scale lateral load tests on a group of bored and a group of driven precast piles were carried out as part of a research project for the proposed high-speed rail system in Taiwan. Standard penetration tests, cone penetration tests (CPT), and Marchetti Dilatometer tests (DMT) were performed before the pile installation. The CPT and DMT were also conducted after pile installation. Numerical analyses of the laterally loaded piles were conducted using *p-y* curves derived from preconstruction and postconstruction DMT and by applying the concept of *p* multipliers. Comparisons between preconstruction and postconstruction CPT and DMT data and evaluation of the results of computations show that the installation of bored piles softened the surrounding soil, whereas the driven piles caused a densifying effect.



## INTRODUCTION

When piles are closely spaced, the individual responses of the piles are influenced by the presence of and load on neighboring piles. In such instances, group action or ''pile-soil-pile interaction'' should be considered. O'Neill (1983) has indicated that the pile-soil-pile interaction consists of ''installation'' and ''mechanical'' effects. Installation effects refer to the alteration of soil stress states, densities, and, perhaps, grain size distributions caused by pile installation, which can be different for groups than for single piles. Mechanical effects refer to the alteration of the soil strains and the failure zones due to simultaneous loading of closely spaced piles. The installation and mechanical effects interact with each other, making a rigorous analysis difficult. Rigidity of the pile cap and the connection of pile to pile cap can also influence the behavior of pile groups. O'Neill (1983) stated that the existing procedures are not likely to provide generally accurate predictions of the distribution of loads to piles in a group because none of the models accounts for the installation effects. As a result, considerable judgment is required to design and analyze closely spaced groups of piles.

Holloway et al. (1981) and Brown et al. (1988) reported that piles in trailing rows of pile groups have significantly less lateral soil resistance than piles in the front row. This is due to the pile-soil-pile interaction that takes place in a pile group. For a given lateral deflection, the lateral resistance of an individual pile in a group is a function of its position in the group and spacing of piles. Brown et al. (1988) suggested that the behavior of each of the individual piles is best modeled by using a family of *p-y* curves. These *p-y* curves can be developed from lateral load tests of a single pile at the test site and modified by reducing the *p* values of all the *p-y* curves on a given pile in the group by a *p* multiplier $f_m$. Experimental data on $f_m$ (Cox et al. 1984; Wang 1986; Brown et al. 1987, 1988; Lieng 1988; McVay et al. 1995) are limited and vary considerably. The available data suggest that the value of $f_m$ is affected by center-to-center pile spacing, relative position with the neighboring piles (i.e., in line, leading, or trailing in a row), pile flexibility, length, and soil conditions. Whether the piles were driven or bored was not considered in selecting the $f_m$ values.

As part of an effort to optimize the design of pile foundations for the proposed high-speed rail system in Taiwan, full-scale load tests were performed on two pile groups and companion single piles. One of the pile groups consisted of bored piles, and the other pile group was composed of driven displacement piles. Single pile load tests were performed on bored and driven piles with similar dimensions and construction procedures used for the piles in the groups.

The test site was located near the middle of the southwestern plain of Taiwan, in Taipao Township of Chaiyi County. Subsurface explorations that included cone penetration tests (CPT) and Marchetti dilatometer tests (DMT) were carried out at the test site before the construction of the piles. The same field crew performed a second series of CPT and DMT after construction of the pile groups, through the pile caps. Comparisons between preconstruction and postconstruction CPT and DMT data allowed the effects of installation on the properties of soil surrounding the piles and behavior of laterally loaded pile groups to be studied.

Five sets of baseline *p-y* curves based on DMT data were used in the analyses of laterally loaded single piles and pile groups. The first two sets of baseline *p-y* curves were computed from preconstruction DMT. These baseline *p-y* curves should reflect the influence of site conditions only, with no consideration of the effects of pile construction methods. The third and fourth sets of baseline *p-y* curves were based on postconstruction DMT performed within the bored pile group. The fifth set of baseline *p-y* curves were derived from postconstruction DMT performed within the driven pile group. The last three sets of baseline *p-y* curves are expected to be affected by the site conditions and the specific pile group installation methods.

Commercial computer codes were used to compute the pile deflection profiles of the single piles and pile groups tested in the field, using the baseline *p-y* curves. None of the baseline *p-y* curves yielded reasonable predictions of pile deflection profiles for the cases analyzed initially. A trial-and-error scheme was then used to match the computed pile deflections with field measurements by multiplying all *p* values of the baseline *p-y* curves by a constant adjustment factor. A unique adjustment factor was determined for each single pile tested, and separate adjustment factors were determined for all piles in each pile group tested. The absolute value of an adjustment factor was intended to account for all the deficiencies in providing the ''correct'' *p-y* curves from DMT for the test site, assumptions related to the structural properties of the piles and rigidity of the connections of pile to pile cap, where applicable, as well as the effects of pile installation. Because of these complications, no further interpretation was made on the basis of the individual adjustment factors. Instead, the installation effects were inferred from comparisons among the adjustment

[1]Prof., Dept. of Civ. Engrg., Nat. Chiao Tung Univ., Hsin Chu 300, Taiwan.
[2]Grad. Res. Asst., Dept. of Harbor and River Engrg., Nat. Taiwan Oc. Univ., Keelung 202, Taiwan.
[3]Prof., Dept. of Civ. Envir. Engrg., Univ. of Houston, Houston, TX 77004.
[4]Prof., Dept. of Harbor and River Engrg., Nat. Taiwan Oc. Univ., Keelung 202, Taiwan.
[5]Prof., Dept. of Civ. Engrg., Nat. Taiwan Univ., Taipei 100, Taiwan.

Note. Discussion open until October 1, 2001. To extend the closing date one month, a written request must be filed with the ASCE Manager of Journals. The manuscript for this paper was submitted for review and possible publication on June 3, 1999; revised December 20, 2000. This paper is part of the ***Journal of Geotechnical and Geoenvironmental Engineering***, Vol. 127, No. 5, May, 2001. ©ASCE, ISSN 1090-0241/01/0005-0385–0397/$8.00 + $.50 per page. Paper No. 21165.



J. Geotech. Geoenviron. Eng. 2001.127:385-397.

factors from computations. This paper presents details of the analyses and discusses the group effects as they relate to the specific site conditions and types of piles involved in this field experiment.

## CONSTRUCTION AND LOAD TESTS OF PILES

A total of 13 cast-in-place bored piles and 13 precast concrete (PC) driven piles were installed at the test site. The ratio of center-to-center spacing between piles over pile diameter ($s/D$ ratio) was 3 for the piles in the group. The location of the test piles in relation to the pile caps and loading devices are shown in Fig. 1. No ground surface movement was monitored during pile installation.

The PC piles were round and hollow, prestressed, and centrifugally cast in 17-m-long segments in a factory. The bottom segment had a closed, pointed steel shoe. A steel ring was attached at the segment ends to facilitate pile splicing by welding the steel rings. A Delmag D-100-13 diesel hammer with a rated energy of 333 kJ was used to drive the PC piles, without penetration aid. The location and verticality of installed PC piles were optically surveyed. No piles had an inclination in excess of 2% of the pile length. The center of each PC pile head was within 2% of the pile diameter from its design location. Strain gauged steel bars and inclinometer casings that extended to the full length of the piles were placed in the void inside the PC pile after driving and then concreted in place. Locations of these instruments are shown in Fig. 2. Structural properties of the hollow PC piles and the concrete infill are shown in Table 1. The PC piles were driven during the period of December 14–18, 1996. Fig. 3 depicts the driving blow counts of all the PC piles. The PC piles shown in Figs. 1 and 3 are numbered according to their driving order (P1 was installed first).

Bored piles were drilled under bentonite slurry (reverse circulation) except for B11–B13. The boreholes of B11–B13 were advanced with a full-length hydraulic oscillator-driven casing. When the casing method was used, the cuttings were removed by a bucket from the inside of the casing. After advancing to the designated elevation, the borehole bottom was cleaned using the bucket. Concrete was placed with a tremie pipe from the bottom of the borehole upward, flushing out the slurry. The casing was gradually removed as the tremie concrete was placed. The center location and verticality of the casing were optically surveyed before concreting.

For bored piles constructed using the reverse circulation method, no temporary casing was used. The borehole dimensions were measured using a ''sonic method'' (Lin and Hoe 1998) upon drilling. The sonic method provided the diameter profile and verticality of the borehole. The center location of each pile head was optically surveyed. The same construction tolerances as described above for PC piles were set for the bored piles and maintained. The installation dates for the bored piles were January 6–29, 1997. The bored piles shown in Fig. 1 are numbered according to their installation order. Structural properties of the bored piles are shown in Table 1. The same tremie concrete placement procedure for the oscillated casing piles were followed, except that there was no casing involved in the construction of reverse circulation piles.

For the bored piles, the strain gauges and inclinometer casings were attached to the longitudinal bars of the reinforcement cage that was inserted before concrete placement. Locations of the strain gauges and inclinometer casings are included in Fig. 2.

Details of the pile-cap connections for the bored and PC pile groups are shown in Fig. 4. The majority of the strain gauges installed in PC and bored piles were damaged during construction. As a result, the lateral deflection profile of piles

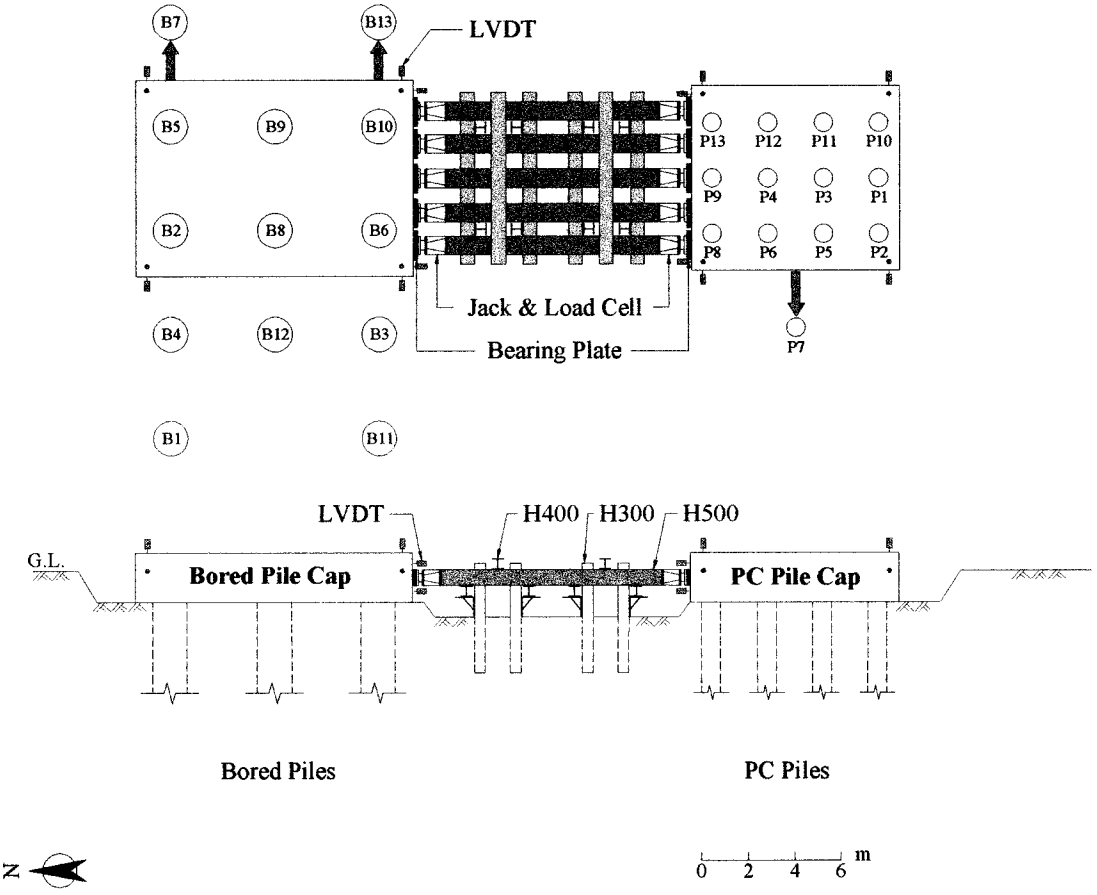


**FIG. 1.** Arrangement of Test Site (G.L. = Ground Level)



J. Geotech. Geoenviron. Eng. 2001.127:385-397.

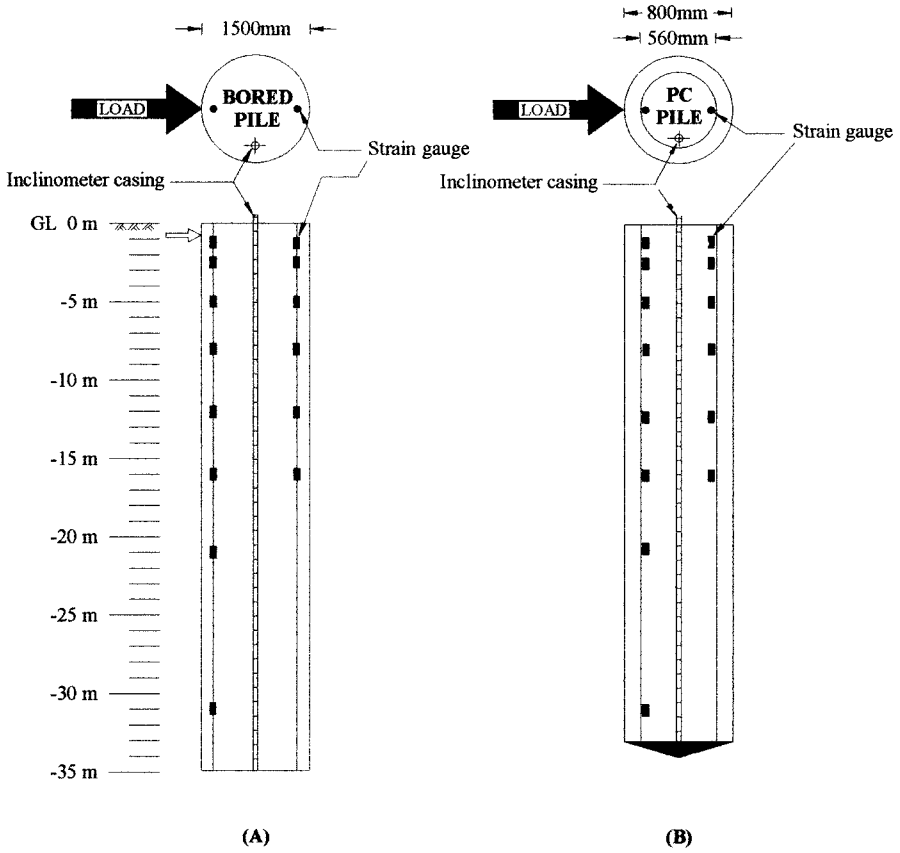


**FIG. 2.** Pile Instrumentations

**TABLE 1.** Structural Properties of Test Piles

| Item | Bored piles | Driven piles |
|---|---|---|
| Pile diameter $D$ (mm) | 1,500 | Precast 800 outside, 560 inside, with concrete infill |
| Pile length (m) | 34.9 | 34.0 |
| Cross-sectional area ($cm^2$) | 17,672 | Hollow: 2,564<br>Solid: 5,027 |
| Concrete compressive strength $f'_c$ (MPa) | 27.5 | Precast: 78.5<br>Infill: 20.6 |
| Reinforcement | | |
| Yield stress $f_y$ (MPa) | 471 | Precast: 1,226<br>Infill: 471 |
| Steel ratio $\rho_s$ | 0.025 | Precast: 0.03<br>Infill: 0.0172 |
| Effective prestress transferred to concrete $f_{ce}$ (MPa) | None | 8 |
| Intact flexural rigidity $EI$ ($GN\text{-}m^2$) | 6.86 | 0.79 |

Note: $EI$ considers solid cross section and effects of steel reinforcement. In case of driven PC piles, $EI$ considers hollow precast, concrete infill, and reinforcement.

during the load test was determined entirely from inclinometer readings.

Axial compression load tests were performed on single piles B8, B9, B12, P3, P4, and P9. Results of the axial load tests on B9 and P3 were used to define the axial load-displacement curves in the analysis of laterally loaded pile groups. Other details of the axial load tests will not be presented because the paper concentrates on lateral load tests. Lateral load tests were conducted on single piles B7, B13, and P7, by loading the piles against the adjacent pile caps (Fig. 1), between May 29 and 31, 1997. Load tests on the two pile groups, 6 bored piles in one group and 12 driven piles in another, were performed by pushing the two pile caps away from each other. The pile group load tests were conducted between June 26 and 28, 1997. A total of 10 pairs of 5-MN hydraulic jacks and load cells were used to apply the lateral forces. Twenty-four LVDTs distributed around the two pile caps were used as the primary means to monitor lateral displacement and rotation in the horizontal and vertical planes (Fig. 1). All measurements were recorded digitally with a computer data logging system.

## SITE CONDITIONS AND IN SITU TESTING PROGRAM

The test site was located within a sugarcane field. The soil depth was >100 m. Subsurface exploration and testing programs were carried out before the pile installations. Eight boreholes extending to a maximum depth of 80 m were drilled at the test site. Soil samples were taken and laboratory tests were performed on the samples. Besides the standard penetration tests performed in sample boreholes, three profiles of CPT and two profiles of DMT were made. Two of the cone penetration test profiles included seismic shear wave velocity measurements [seismic cone penetration tests (SCPT)]. Boring and in situ test locations are depicted in Fig. 5.

Fig. 6 reports profiles of preconstruction standard penetration tests blow counts $N$ (blows per 0.3-m penetration), DMT liftoff $P_0$ and 1.1-mm expansion $P_1$ pressure, material index $I_D$, fines content, and maximum shear modulus $G_{max}$ from the SCPT. The value of $I_D$, dilatometer modulus $E_D$, and stress index $K_D$ were determined based on values of $P_0$ and $P_1$

$$I_D = \frac{P_1 - P_0}{P_0 - u_0} \tag{1}$$

$$E_D = 34.7(P_1 - P_0) \tag{2}$$

$$K_D = \frac{P_0 - u_0}{\sigma'_v} \tag{3}$$



J. Geotech. Geoenviron. Eng. 2001.127:385-397.

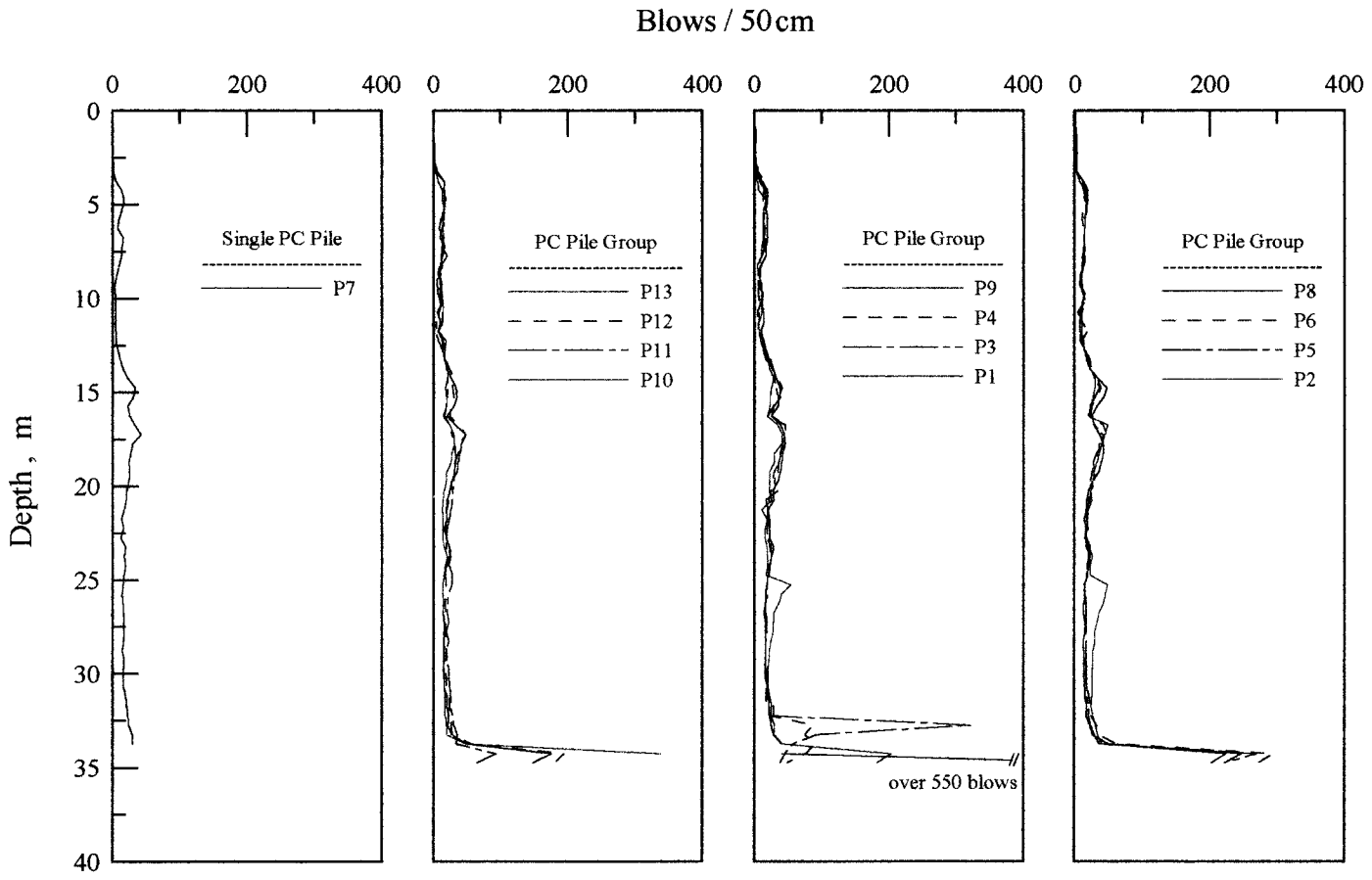


**FIG. 3.** Blow Counts of Driven Piles

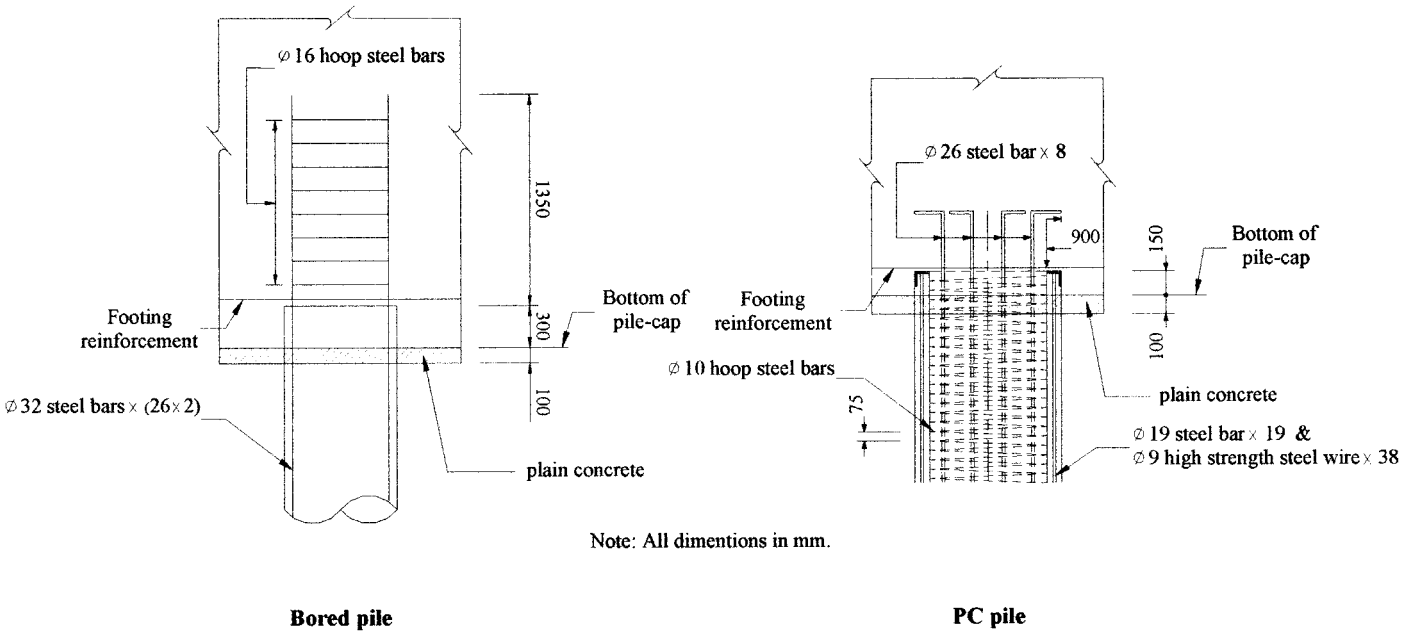


**FIG. 4.** Details of Pile-Cap Connections

where $u_0$ = hydrostatic pressure prior to dilatometer penetration; and $\sigma'_v$ = effective vertical stress prior to dilatometer penetration. Depending on the fines content, the soils within the 80 m depth were generally classified as silty sand (SM) or silt (ML) with occasional layers of silty clay (CL), according to soil samples recovered in the borings.

Variations in the available field test data from different locations were small, indicating relatively uniform soil conditions at the test site. The ground-water table was located at approximately 1 m below the ground surface and did not vary significantly over the course of the project.

## EFFECTS OF PILE INSTALLATION ON STATE OF SURROUNDING SOIL

Plastic pipes were cast in the pile caps to facilitate CPT and DMT after construction. Two profiles of DMT (numbered



J. Geotech. Geoenviron. Eng. 2001.127:385-397.

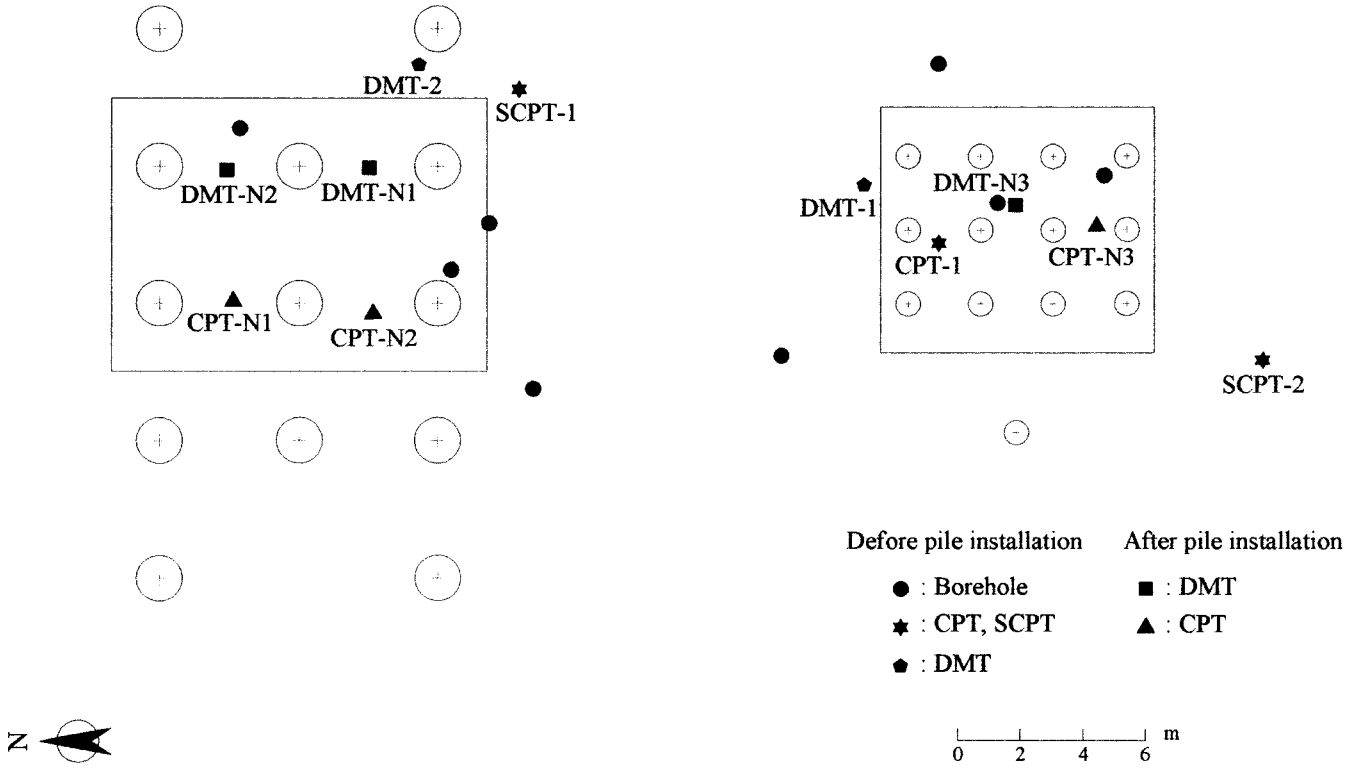


**FIG. 5.** Boring Location Diagram

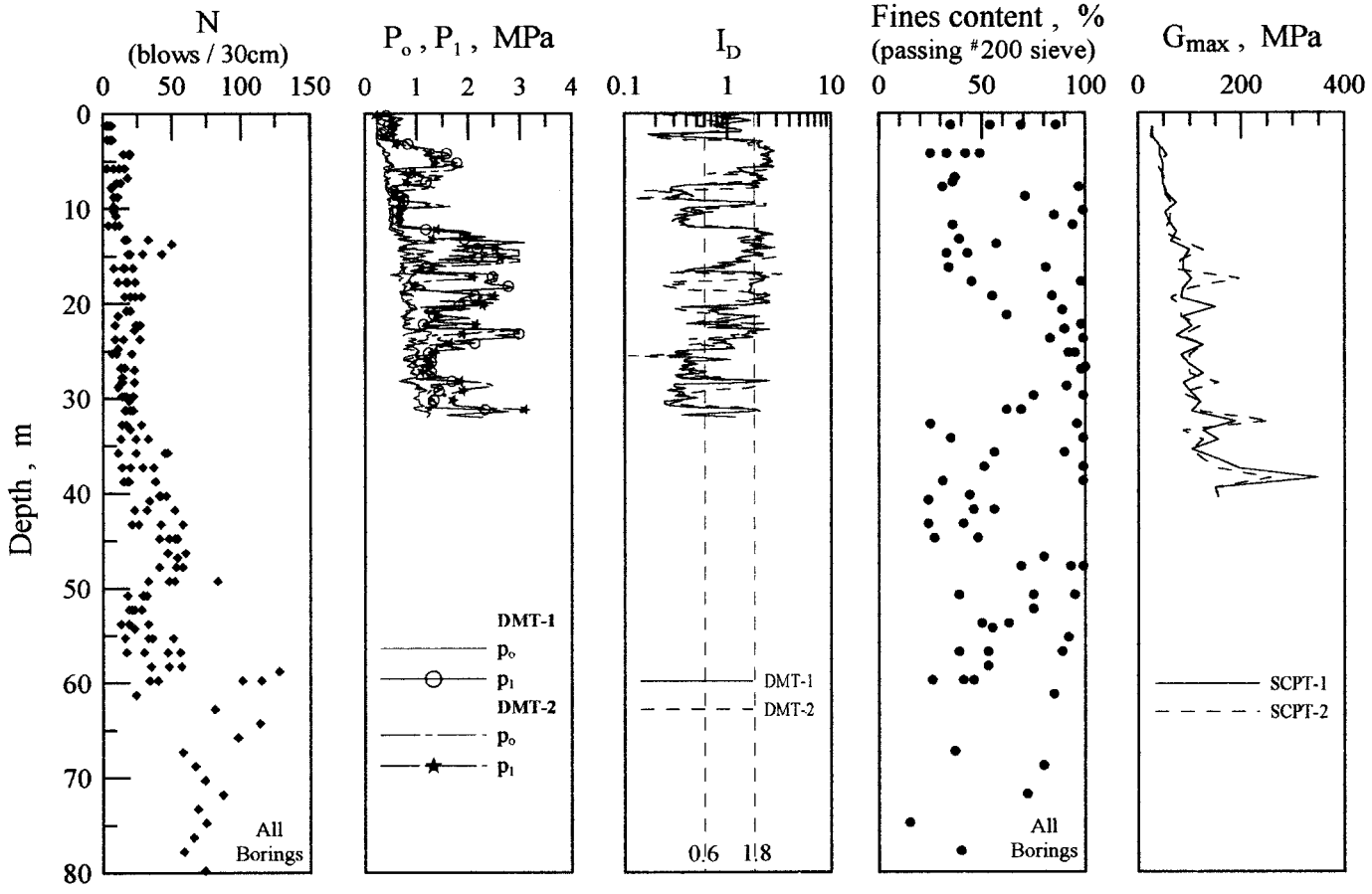


**FIG. 6.** Soil Profiles



J. Geotech. Geoenviron. Eng. 2001.127:385-397.

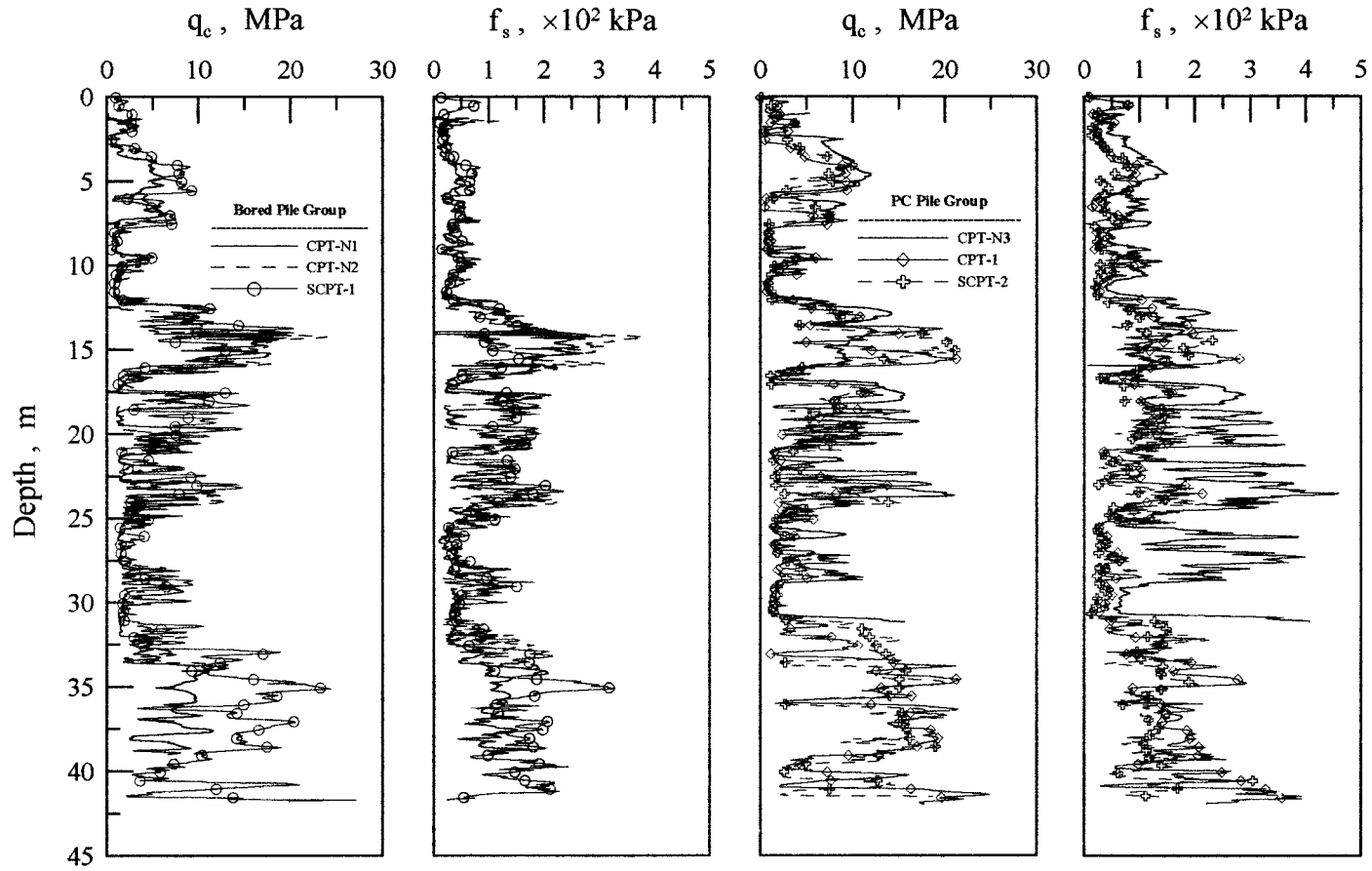


**FIG. 7.** Comparison of CPT Profiles

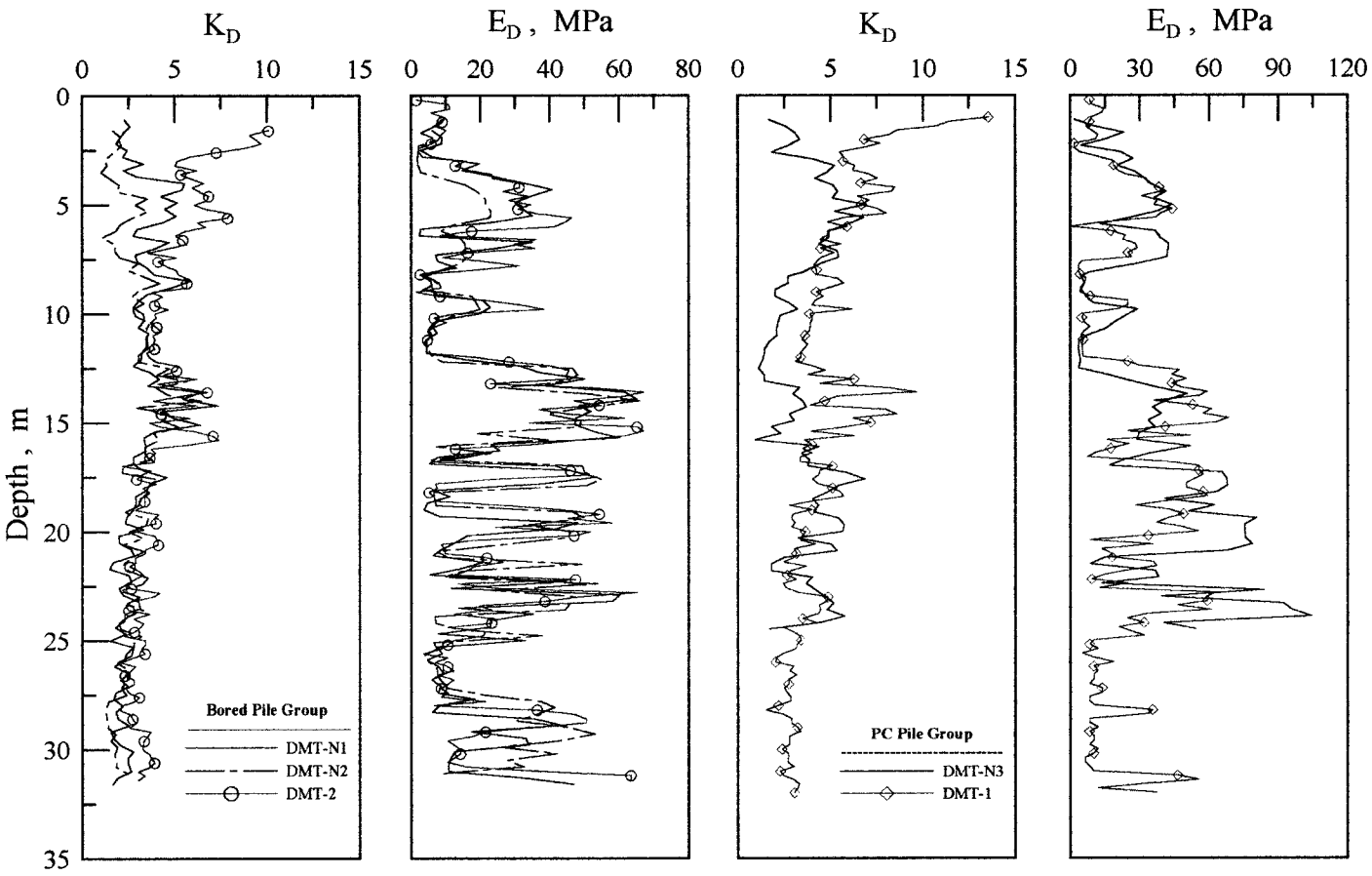


**FIG. 8.** Comparison of DMT Profiles



J. Geotech. Geoenviron. Eng. 2001.127:385-397.

DMT-N1 and DMT-N2 in Fig. 5) and CPT (CPT-N1 and CPT-N2) were measured through the bored pile cap. One profile of DMT (DMT-N3) and CPT (CPT-N3) were measured through the driven pile cap. The postconstruction in situ tests were conducted before the lateral load tests. The preconstruction and postconstruction cone tip resistance $q_c$ and sleeve friction $f_s$ from the CPT are compared in Fig. 7. Values of $K_D$ and $E_D$ from the preconstruction and postconstruction DMT are depicted in Fig. 8. Note that the depth in Figs. 7 and 8 are in reference to the original ground surface. Postconstruction penetration tests started at 1 m below the original ground surface, where the bottom of the pile cap was located. In most cases there were two profiles of either preconstruction or postconstruction CPT or DMT. This arrangement helps in clarifying whether the differences between the preconstruction and postconstruction tests were part of the soil heterogeneity or effects of pile group installation.

The value of $q_c$ is known to increase with density (Jamiolkowski et al. 1988) of sand or undrained shear strength of clay (Campanella and Robertson 1988). For CPT in sand, the magnitude of effective stress also affects $q_c$; however, there is no generally acceptable conclusion as to which component of the state of stress (i.e., vertical, horizontal, or mean normal stress) should relate to $q_c$ (Huang and Ma 1994). For the same stress conditions in sand, a higher $f_s$ is expected to be associated with higher density. Briaud and Miran (1992) reported that, for a given ratio of $q_c/\sigma'_v$, the coefficient of earth pressure at rest $K_0$ increases with $K_D$. For the same $K_D$, $K_0$ decreases with $q_c/\sigma'_v$. For DMT in sand, the relationships between $K_D$ and $K_0$ are qualitative in nature. For a given material index $I_D$, $E_D$ increases with the rigidity or density of soils. The construction of piles is not likely to alter the vertical stress or the type of soil at the postconstruction DMT locations. Thus, $\sigma'_v$ and $I_D$ should remain the same after the pile group installation.

As will be presented later, the majority of lateral displacements occurred within the top 10 m of the test piles. Thus, variations of CPT and DMT data in this depth range should be of major concern. According to Fig. 7, there were distinct and significant decreases of $q_c$ and $f_s$ at depths of 3–7.5 m as a result of bored pile group installation. The construction of the driven PC pile group caused increases of $q_c$ and $f_s$ at depths from 2.5 to 6 m. The DMT data reported in Fig. 8 show that the construction of both bored and PC piles caused decreased $K_D$ within the top 5–6 m. For PC piles, decreases in $K_D$ were also noticed at depths of 7.5–15 m. The value of $E_D$ remained more or less the same in both cases. The changes of CPT and DMT data, for the remaining test depth, were not significant or consistent enough to be conclusive. Based on available experience in interpreting CPT and DMT as described above, importance of test data from the top 10 m, and available test results, it can be concluded that the construction of bored and PC pile groups had its most apparent effects on the state of the soils surrounding the piles above a depth of 15 m. Because of prior water table fluctuations and surface desiccation, the near-surface soils were a crustlike material in an overconsolidated state that possesses a higher $K_0$ than at greater depths. Apparently, the construction of piles, bored and driven, tended to disrupt this crust and caused $K_0$ to decrease, thus lowering $K_D$ values. There is no conclusive evidence, at least from the interpretation of $E_D$, to indicate a trend in the change of soil stiffness as a result of bored or driven pile group installation. According to CPT, the construction of bored piles had a loosening effect on the surrounding soil down to a depth of approximately 6 m. The reduction of density coupled with a loss of $K_0$ would have caused the soil to reduce its capacity in resisting lateral load within the bored pile group. The construction of driven PC piles apparently had densified the surrounding soil, which offset the effects of reducing $K_0$. The net effects on the laterally loaded PC pile group are not immediately clear without further analysis.

## ANALYSIS OF SINGLE LATERALLY LOADED PILES USING DMT DATA

Piles B7 (bored) and P7 (driven) served as reference single piles to establish the *p-y* curves for the analysis of laterally loaded pile groups. These single piles were analyzed using the two sets of baseline *p-y* curves inferred from preconstruction DMT, made closest to the reference piles (DMT-2 for B7 and DMT-1 for P7). Pile B13 was constructed using the casing method, which was not used for the construction of the bored piles in the group. Therefore, B13 was not selected as a reference single pile, although B13 was closer to DMT-2 than B7. The computer code LPILE (Reese and Wang 1993) was used to perform the computations. The single-pile load tests were conducted with no constraint on the pile head (head moment = 0). For LPILE computation, zero lateral soil resistance was assumed at the ground surface. The lateral load was applied at the ground surface in LPILE computations, as was the case in field tests. Piles B7 and P7 were laterally loaded in cycles. Results of the measured head deflection versus load are shown in Fig. 9. A constant *EI* representing an intact pile, as shown in Table 1, was used initially in the computations. The field inclinometer measurements indicated a sharp change in curvature in B7 at 7–10 m below the ground surface when the lateral load exceeded 1,462 kN. The same effect was observed in P7 at depths between 4.5 and 5 m as the lateral load reached 570 kN. Most likely, the piles cracked at these depths. Reduced *EI* values were assigned to part of the piles to reflect the influence of section cracking, as shown in Table 2.

The *p-y* curves required for the analysis of laterally loaded piles were established using DMT data, according to the procedure proposed by Robertson et al. (1989). The *p-y* curve was assumed to follow the shape suggested by Matlock (1970)

$$\frac{p}{p_u} = 0.5(y/y_c)^{0.33} \quad \text{for } y \leq 8y_c \tag{4a}$$

$$p = p_u \quad \text{for } y > 8y_c \tag{4b}$$

where $p$ = soil lateral resistance per unit length of pile; $p_u$ = ultimate soil lateral resistance per unit length of pile; $y$ = lateral deflection of the pile element; and $y_c$ = lateral deflection of the pile element corresponding to $p = 0.5p_u$.

The computation of *p-y* curves started at a $y$ value equal to $0.1y_c$. In addition to $E_D$, $I_D$, and $K_D$, the values of $p_u$ and $y_c$ depended on the selection of empirical constants $F_c$(= 10), $F_\phi$(= 1.0), and $J$(= 0.5). Readers are referred to Robertson et al. (1989) for details. The piles were divided into 300 equally long segments for LPILE computations. The $p_u$ and $y_c$ values used in the LPILE analysis are plotted in Fig. 10.

A similar procedure was followed to develop postconstruction *p-y* curves from the ''N'' series of DMT. However, DMT-N3 terminated at 25 m. The postconstruction $p_u$ and $y_c$ values for PC piles at 25–35 m were based on DMT-1, the same as those used in the preconstruction *p-y* curves. This substitution is not expected to have significant effect on LPILE computations, as the majority of pile deflections occurred within the top 10 m.

The resulting analyses did not match the measurements because the initial *p-y* curves based on preconstruction DMT were apparently not completely appropriate for the site and construction conditions. The DMT preconstruction *p-y* curves were therefore modified by adjusting all the $p$ values along each curve. This modification was done by multiplying all the $p$ values by a single pile adjustment factor $p_{ms}$. The two reference piles were analyzed with the ''adjusted'' *p-y* curves



J. Geotech. Geoenviron. Eng. 2001.127:385-397.

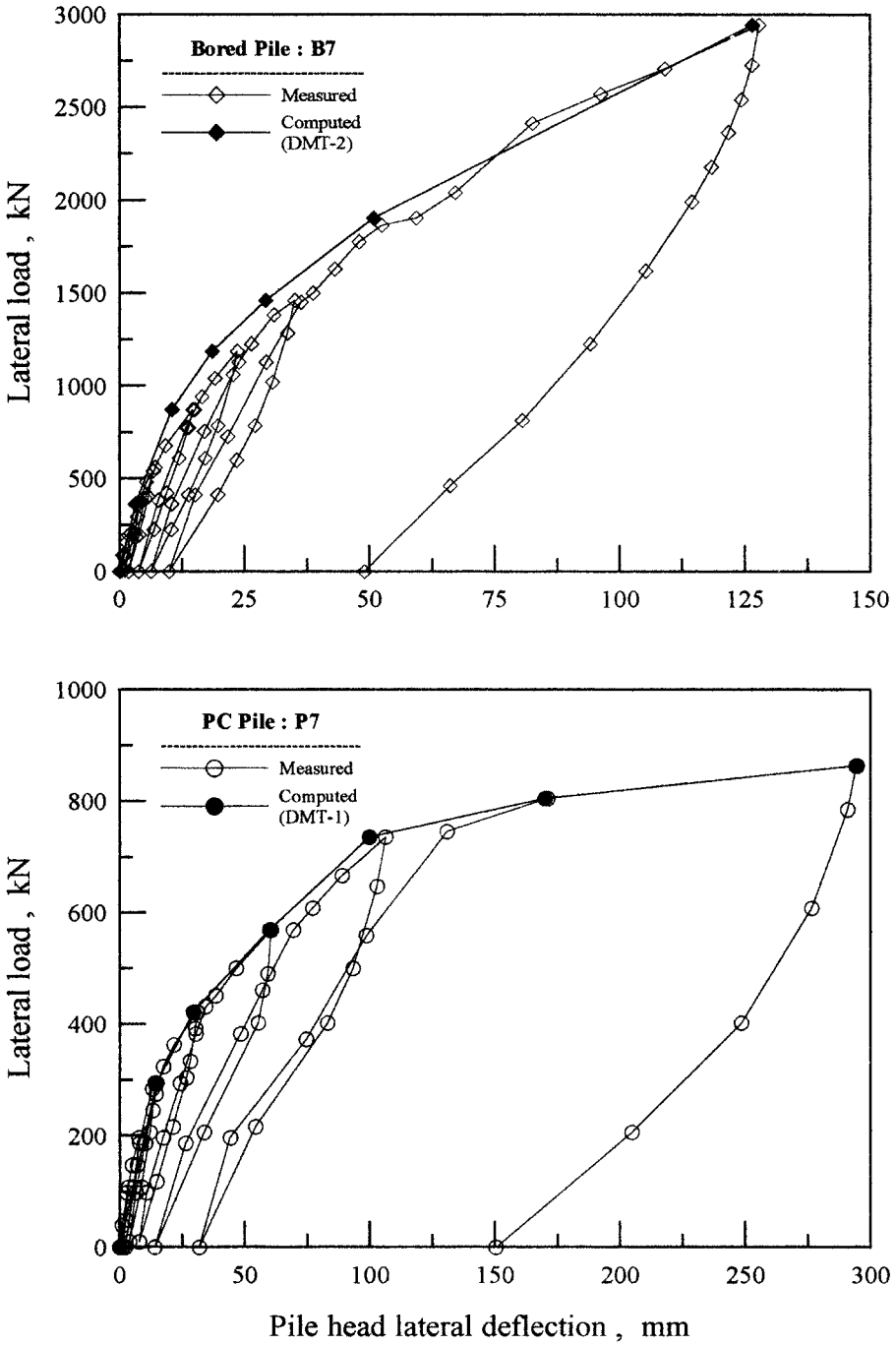


**FIG. 9.** Single Pile Lateral Load versus Head Deflection

using LPILE by successively varying $p_{ms}$ until a match between the measured and computed pile load-deflection profiles was achieved. The $p_{ms}$ values determined for B7 and P7 were 0.50 and 0.21, respectively. The resulting *p-y* curves ($p_u$ and $y_c$ obtained from the DMT, and with all the *p* values multiplied by $p_{ms}$) were accepted as the calibrated, site-specific *p-y* curves for the respective bored and driven piles, acting individually at the site. This set of *p-y* curves considers the effects of single pile construction at the particular site.

Comparisons between the computed and measured pile deflection profiles and moment distribution from LPILE computations with the modified preconstruction *p-y* curves are depicted in Fig. 11. The computed pile deflections in Fig. 11 and those shown in Fig. 9 were generally within 10% of the measured values for both piles, under all loads.

## ANALYSIS OF LATERALLY LOADED PILE GROUPS

Because of the relative rigidity of the reaction frame placed between the bored and PC pile caps (Fig. 1), the lateral load sustained by the PC pile group was not the same as that sustained by the bored pile group. That is, the reaction frame carried a small fraction of the lateral load. According to LVDT readings taken during the pile group load test, the PC and bored pile caps had a maximum torsional movement in the horizontal plane of 0.08° counterclockwise and 0.006° clockwise, respectively. The inner side of bored and PC pile caps, where the pile caps met the load frame, were lifted slightly during the pile group load test. The lifting caused the two pile caps to rotate away from each other in the vertical plane, with a maximum rotation of 0.03° (bored pile cap) and 0.06° (PC pile cap).



J. Geotech. Geoenviron. Eng. 2001.127:385-397.

**TABLE 2.** Flexural Rigidity Values Used in Single Pile Analyses

| Lateral load (kN) | 7 m ≤ $x$ ≤ 10 m | Rest of pile |
|---|---|---|
| | (a) $EI$ of B7 (GN-m$^2$) | |
| 363 | 6.86 | 6.86 |
| 814 | 6.86 | 6.86 |
| 1,148 | 6.86 | 6.86 |
| 1,462 | 5.75 | 6.86 |
| 1,903 | 4.29 | 6.86 |
| 2,943 | 4.29 | 6.86 |
| | (b) $EI$ of P7 (GN-m$^2$) | |
| 265 | 0.79 | 0.79 |
| 422 | 0.79 | 0.79 |
| 570 | 0.14 | 0.79 |
| 736 | 0.10 | 0.79 |
| 804 | 0.05 | 0.79 |
| 863 | 0.02 | 0.79 |

The analysis for the pile group was conducted using the "GROUP" computer program (Reese and Wang 1996). The unit axial load transfer curves (often referred to as the $t$-$z$ curves) were generated internally by GROUP, based on single pile axial load test results of B9 and P3 for bored and driven PC piles, respectively. The axial load-displacement measurements of B9 and P3, from axial load tests, are shown in Table 3. According to Reese and Wang (1996), the value of $p_u$ for the pile in question is reduced by a $p$ multiplier $f_m$, without direct consideration of how displacements $y$ are affected. It is obvious from (4) that, if $p_u$ is reduced, $p$ is also reduced at every point on the $p$-$y$ curve and soil stiffness is therefore also reduced. The value of $f_m$ depends on the group geometry, particularly the relative pile spacing $s/D$. For the two test pile groups shown in Fig. 1 ($s/D$ = 3), the values of $f_m$ based on empirical equations given by Reese and Wang (1996) are shown in Table 4. The equations suggested by Reese and Wang (1996) are based on small-scale experiments performed on several sets of pile groups in different types of soil.

There was no apparent sign of pile breakage (no sudden changes in measured curvature) during the load test. The amount of pile-cap rotations in the vertical plane as previously described was relatively small. Thus, the pile-cap rotation induced axial stress within the group piles is not expected to be high enough to cause cracking. For these reasons, the intact (uncracked) $EI$ values for bored and PC piles shown in Table 1 were used in the GROUP computations, regardless of the level of lateral load. The pile group analyses were divided into two stages. In the first stage, the baseline $p$-$y$ curves from preconstruction DMT (DMT-1 for PC pile group and DMT-2 for bored pile group) were applied, without using the single pile adjustment factor $p_{ms}$. To account for the group effects and to facilitate matching between the computed and measured pile group deflection-load relations, two modification factors $f_m$ and $p_{mga}$ were introduced into the group-pile $p$-$y$ curves

$$\frac{p}{p_u} = p_{mga} f_m 0.5 \left(\frac{y}{y_c}\right)^{0.33} \tag{5}$$

in which $f_m = p$ multiplier recommended by Reese and Wang (1996). The value of $f_m$ was assumed constant for piles in a given row, as indicated in Table 4. In principle, $f_m$ is strictly a function of geometry; it makes no difference whether the piles were bored or driven. The additional adjustment factor $p_{mga}$ serves to distinguish between the group construction effects for bored and driven piles. The value of $p_{mga}$ (common for all piles in a given group) was varied until a good match was achieved between the measured and computed pile-cap load-deflection profiles.

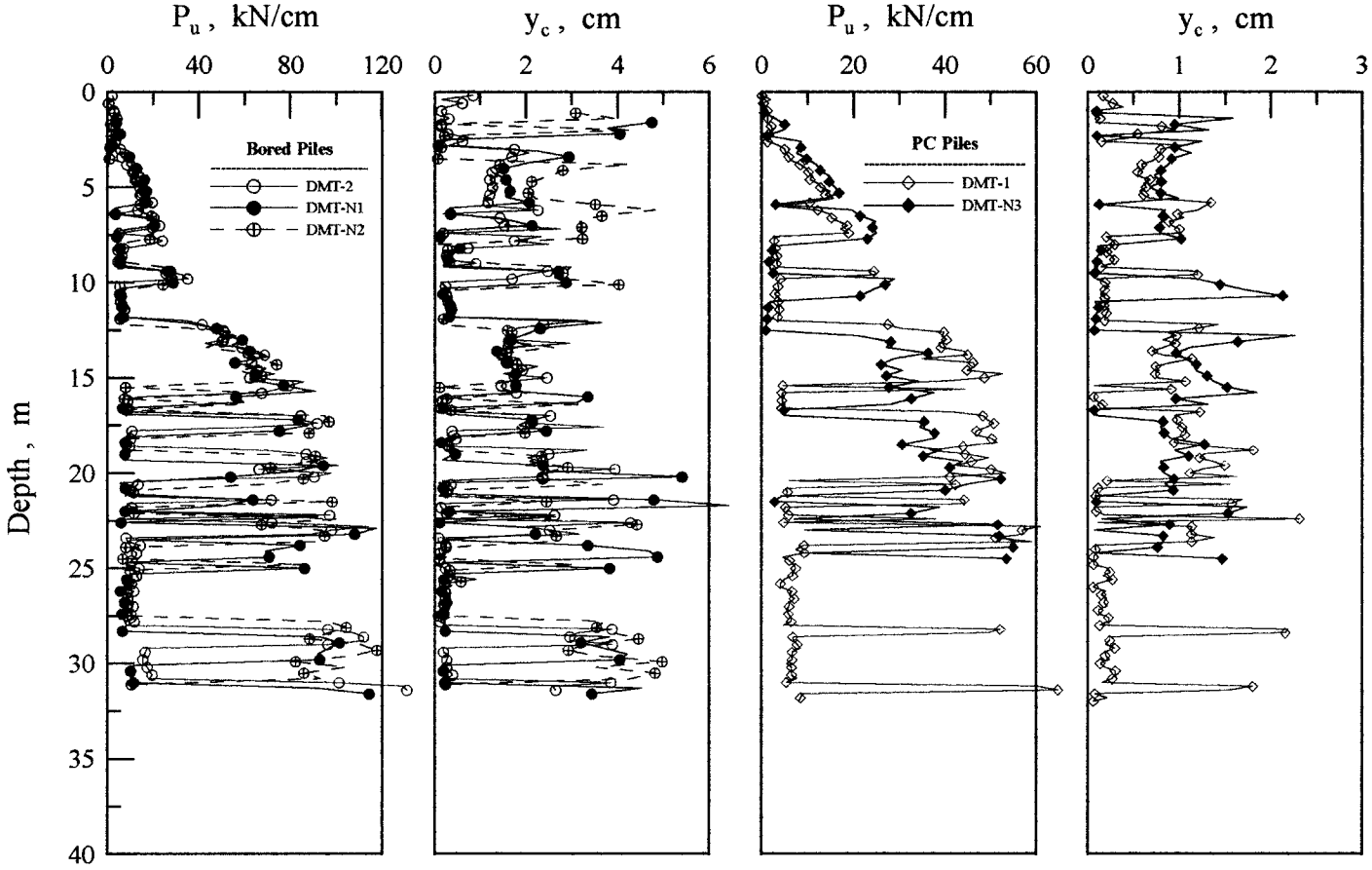


**FIG. 10.** Profiles of $p_u$ and $y_c$ Values



J. Geotech. Geoenviron. Eng. 2001.127:385-397.

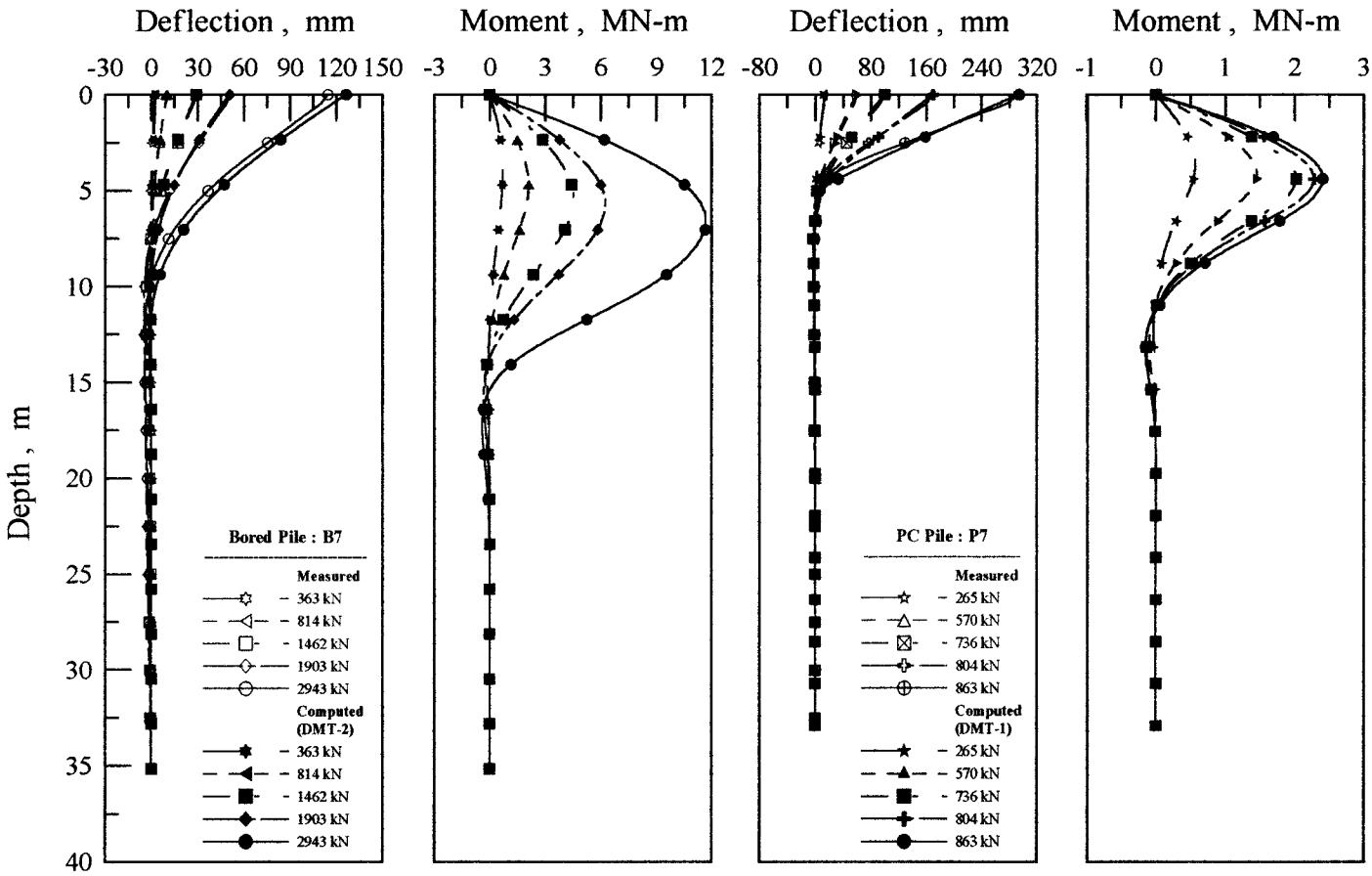


**FIG. 11.** Deflection and Moment Profiles of Single Piles

**TABLE 3.** Axial Load Test Data

| Axial Load Test of B9 | | Axial Load Tests of P3 | |
|---|---|---|---|
| Axial load (kN) | Displacement (mm) | Axial load (kN) | Displacement (mm) |
| 980 | 0.28 | 980 | 0.86 |
| 2,940 | 1.22 | 1,949 | 2.28 |
| 4,900 | 2.52 | 2,947 | 4.13 |
| 6,860 | 4.77 | 3,940 | 6.46 |
| 8,820 | 9.13 | 4,892 | 9.44 |
| 10,780 | 42.61 | 5,857 | 26.76 |
| 12,740 | 102.80 | 6,850 | 69.64 |
| 13,475 | 134.50 | 7,616 | 101.14 |

In the second stage of pile group analyses, the formulation of baseline *p-y* curves was based on postconstruction DMT data. DMT-N1 and DMT-N2 were used independently to determine two sets of $p_u$ and $y_c$ values for the bored piles and the data from DMT-N3 were used for the driven piles. The same set of $f_m$ values shown in Table 4 were applied. The *p-y* curves were modified

$$\frac{p}{p_u} = p_{mgb} f_m 0.5 \left(\frac{y}{y_c}\right)^{0.33} \tag{6}$$

where $p_{mgb}$ served the same purpose as $p_{mga}$, except that the baseline data were obtained from the DMT acquired after pile

**TABLE 4.** Summary of Group Pile Reduction Factors

| Row | Bored group piles $p_{mga} = 0.47$, $p_{mgb} = 0.56$ | | Row | Driven group piles $p_{mga} = 0.37$, $p_{mgb} = 0.26$ | |
|---|---|---|---|---|---|
| | $f_m$ | $p_m$ | | $f_m$ | $p_m$ |
| Leading | 0.932 | 0.876 | Leading | 0.893 | 1.573 |
| Middle | 0.704 | 0.662 | Leading-middle | 0.614 | 1.082 |
| Trailing | 0.740 | 0.696 | Trailing-middle | 0.614 | 1.082 |
| | | | Trailing | 0.660 | 1.163 |
| Load, *kN* | Pile/cap connection *kN – m/rad* | | Load, *kN* | Pile/cap connection *kN – m/rad* | |
| 3414 | Fixed | | 2835 | $4.5\times10^5$ | |
| 6111 | Fixed | | 5337 | $2.3\times10^5$ | |
| 6416 | Fixed | | 5248 | $2.3\times10^5$ | |
| 8348 | Fixed | | 7122 | $1.6\times10^5$ | |
| 9643 | $1.7\times10^7$ | | 8231 | $4.5\times10^4$ | |
| 10948 | $1.7\times10^7$ | | 9251 | $3.2\times10^4$ | |

Note: Reduction factors are for s/D =3.



J. Geotech. Geoenviron. Eng. 2001.127:385-397.

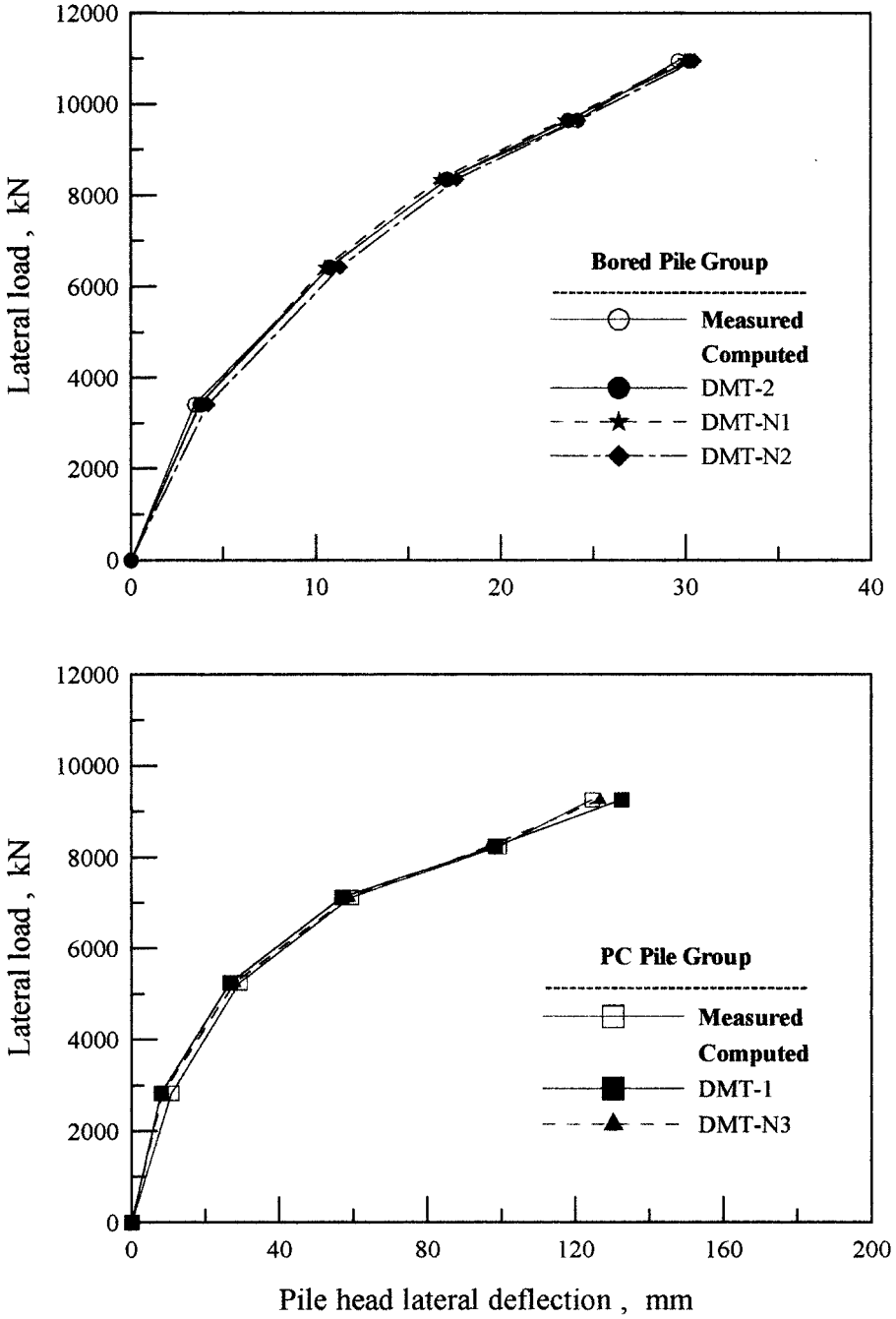


**FIG. 12.** Group Pile Cap Lateral Load versus Deflection

group installation but before loading. The values of $p_u$ and $y_c$ used in (6) are shown in Fig. 10. Again, the value of $p_{mgb}$ (common for all piles in a given group) was varied until a good match was achieved between the measured and computed pile-cap load-deflection profiles. Table 4 shows the values of $p_{mga}$ and $p_{mgb}$ from GROUP computations.

The stiffness of the pile-cap connection has a significant effect on the behavior of pile groups. In the GROUP computations, the stiffness values for the pile-cap connections considered the characteristics of structural members and matching of the computed pile deflection profiles near the connection points with those from inclinometer readings. The assumed stiffness at the connection between piles and the pile cap for GROUP computations are included in Table 4. A rigid connection for bored pile-cap connections was assumed for lateral loadings up to 9,634 kN. Inclinometer readings showed relatively large rotation at the PC pile-cap connections from the beginning of the lateral load test. Thus, the pile-cap connections were assumed to be elastic and rotational stiffness values were selected for GROUP computations for the PC pile group under all applied lateral loads.

The computed pile-cap load-deflection relations using the *p-y* curves defined by (5) and those defined by (6) with the parametric values in Table 4 are compared in Fig. 12 with the measured relations. The two numerical solutions are seen to give essentially equivalent results. For the bored pile group, the computed deflections from DMT-N1 and DMT-N2 are very similar, as indicated in Fig. 12. This similarity of computed results is an indication that the effects of the bored pile group construction as determined by DMT are consistent within the pile cap. The following discussion will involve results from DMT-N1 only, for the bored pile group.



J. Geotech. Geoenviron. Eng. 2001.127:385-397.

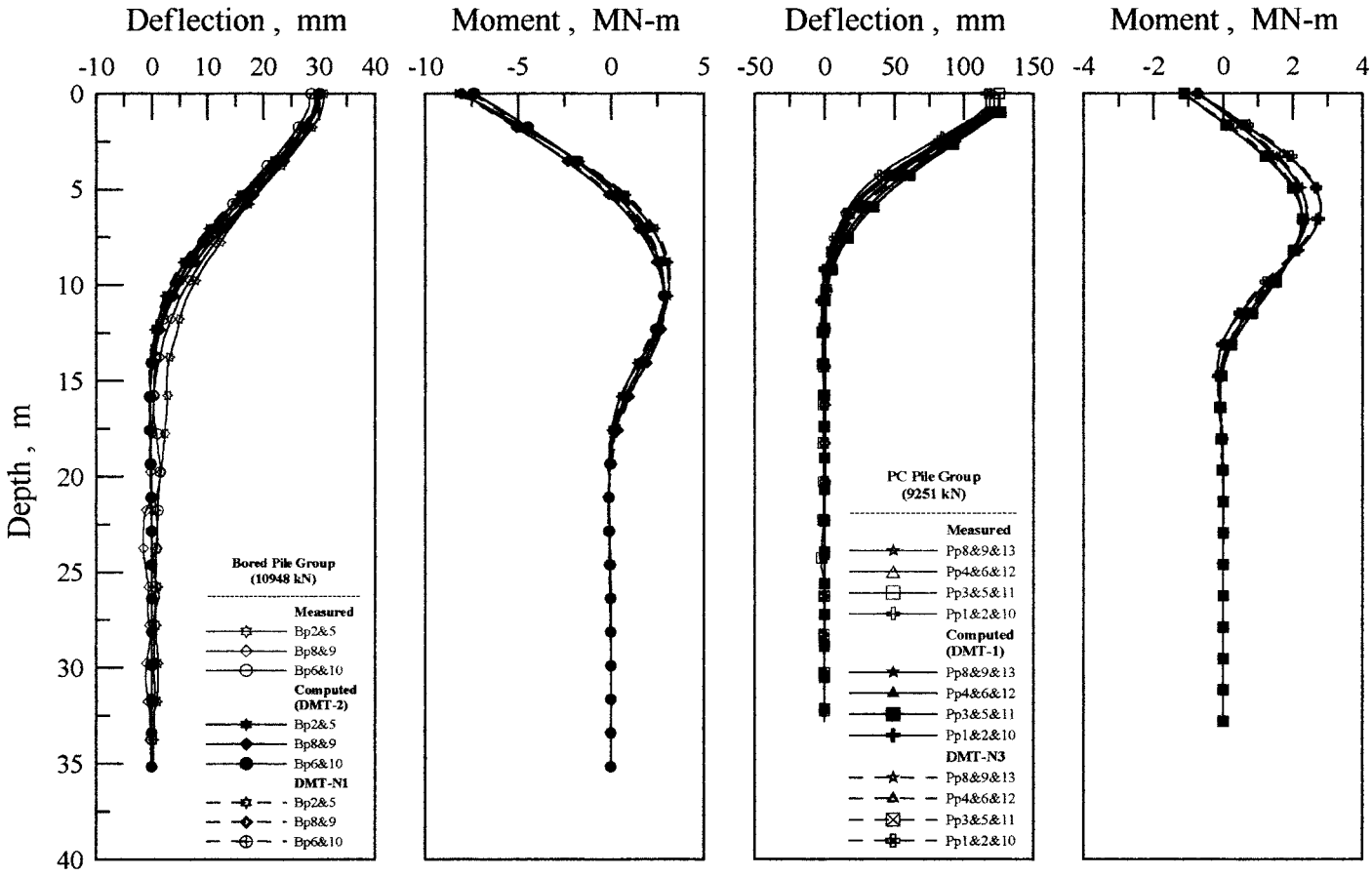


**FIG. 13.** Deflection and Moment Profiles of Group Piles

Fig. 13 depicts the measured deflection profiles, computed deflection, and moment profiles under the maximum applied lateral loads of 10,948 and 9,251 kN for the bored and PC piles, respectively. It is apparent that pile deflection profiles based on preconstruction and postconstruction *p-y* curves [(5) and (6)], with the appropriate values of $p_{mga}$ and $p_{mgb}$, can match the measured profiles equally well. Note that, because of the inevitable errors in orienting the inclinometer casings, some scattering of measured pile deflections was noticeable, as shown in Fig. 13.

In (5), $f_m$ multiplied by $p_{mga}$ reflects the effects of installation of the group piles and pile group loading (installation as well as mechanical effects). Because of the timing and positions of postconstruction DMT, when the *p-y* curves were created according to (6), the product of $f_m$ and $p_{mgb}$ should account mostly for the effects of pile group loading (mechanical effects). Because the same $f_m$ was used in both (5) and (6), the relative values of $p_{mga}$ and $p_{mgb}$ should then reflect mostly the effects of the installation of piles in a group. For bored piles, $p_{mgb}/p_{mga}$ = 1.19, indicating that the installation of the bored pile group softened the soil surrounding the piles. For the driven pile group, $p_{mgb}/p_{mga}$ = 0.70, indicating that the effects of the driven pile group installation was to stiffen the soil surrounding the piles.

## PRACTICAL IMPLICATIONS

In practice, it is rarely possible to perform in situ tests such as DMT after pile installation and through the pile caps, as reported in this paper. Using the single pile analysis as a reference and considering the results obtained in this study, a new pile group *p* multiplier $p_m$ is proposed

$$p_m = f_m \left( \frac{p_{mga}}{p_{ms}} \right) \tag{7}$$

The intention of normalizing $p_{mga}$ with respect to $p_{ms}$ is to nullify the effects of errors in using the DMT as a means to determine the necessary *p-y* curves. The value of $p_m$ may be considered as a site-specific pile group *p* multiplier that reflects group mechanical and installation effects at the Chaiyi test site. The values of $p_m$ were derived separately for bored and driven piles and are shown in Table 4. The values of $f_m$ suggested by Reese and Wang (1996), Brown and Shie (1991), and other authorities, however, do not make such a distinction. The differences between the values of $p_m$ and $f_m$ shown in Table 4 appear to be significant. It should be emphasized that, in addition to *p-y* curves, the results of GROUP analyses were also sensitive to the conditions of the connection between the piles and pile cap and to the axial pile stiffness. Thus, not only do the *p* multipliers relate to soil conditions and installation effects but they are also affected by how the group of piles is modeled. This is the principal reason for the variable nature of the *p* multipliers from previous field studies.

For the driven piles analyzed herein, the values of $p_m$ were 76% higher than those of $f_m$. The installation of the driven pile group is inferred to have caused significant stiffening effects in the soil surrounding the piles. The values of $p_m$ were consistently >1.0. This unusual result may also be related to the fact that the rotational restraint at the pile heads was stiffer than what was modeled in the GROUP analyses. The disregard of any shear force that might have developed along the base of the cap during lateral loading could be another reason for the unusually high $p_m$ values. In other words, the values of $p_m$ are likely to be affected by the specific way in which the pile



J. Geotech. Geoenviron. Eng. 2001.127:385-397.

group was modeled, in addition to soil conditions and the pile construction method. For bored piles, the values of $p_m$ were 6% less than those of $f_m$. In this case, the softening effects to the surrounding soil caused by the installation of bored piles are slightly underestimated by using $f_m$.

In practice, one could analyze similar pile groups at a site with similar soil conditions using GROUP or a comparable program, using the concept of *p* multipliers. The analyses start with the development of *p-y* curves for single piles, for example, by using DMT obtained prior to pile installation. The best estimate preconstruction *p-y* curves are then modified by multiplying all *p* values by $p_m$ for the pile group analysis. The selection of $p_m$ considers the group geometry and the type of piles (bored or driven) similar to those considered in Table 4. To match the pile-deflection profiles computed by GROUP with the measurements, substantial adjustment on the rigidity of the pile-cap connection was necessary, as previously described. The adjustment apparently had significant impact on the result of the computations. Other modeling techniques or computer codes may use different methods for simulating the pile-cap connection conditions and thereby result in different *p* multipliers. Therefore, the values of $p_m$ given in Table 4 are appropriate only for an analysis procedure similar to that, which was followed in this paper.

## CONCLUDING REMARKS

The CPT and DMT performed within the pile caps offered an opportunity to evaluate the construction effects on the behavior of laterally loaded pile groups. For the case studied, the pile group installation, bored or driven, tended to disrupt a crustlike material near the ground surface and lower the in situ lateral stress. Bored pile group construction appeared to loosen the soil surrounding the piles, whereas the driven pile group construction apparently caused a densifying effect. The construction effects were limited to the top 15 m from ground surface, where soil conditions have the greatest effect on the behavior of laterally loaded piles.

The *p*-multiplier values reported by various authors inherently combine the mechanical effects with the installation effects and do not distinguish between driven displacement piles and bored piles. The study reported above has indicated that the lateral soil resistance against piles in a group can be highly dependent on the type of pile installation (driven or bored) and preconstruction soil conditions. It is not simply a matter of geometry as typically assumed in current practice. Separation of mechanical effects from installation effects is likely to result in more consistent *p* multipliers. Specific *p* multipliers $p_m$ for concrete piles are also likely a function of how the nonlinear bending of the piles is modeled, how the axial stiffness is modeled, and how the connectivity between the piles and pile cap is simulated. Therefore, the values of $p_m$ given in Table 4 are appropriate only for an analysis procedure and pile group tested configuration similar to those described in this paper.

## REFERENCES


Briaud, J. L., and Miran, J. (1992). "The flat dilatometer test." *Rep. No. FHWA-SA-91-44*, Federal Highway Administration, Washington, D.C.

Brown, D. A., Morrison, C., and Reese, L. S. (1988). "Lateral load behavior of pile group in sand." *J. Geotech. Engrg.*, ASCE, 114(11), 1261–1276.

Brown, D. A., Reese, L. C., and O'Neill, M. W. (1987). "Cyclic lateral loading of a large-scale pile group." *J. Geotech. Engrg.*, ASCE, 113(11), 1326–1343.

Brown, D. A., and Shie, C. F. (1991). "Modification of *p-y* curves to account for group effects on laterally loaded piles." *Geotechnical engineering congress, Geotech. Spec. Publ. No. 27*, ASCE, New York, 479–490.

Campanella, R. G., and Robertson, P. K. (1988). "Current status of the piezocone test." *Proc., 1st Int. Symp. on Penetration Testing, ISOPT-1*, Vol. 1, J. de Ruiter, ed., Balkema, Rotterdam, The Netherlands, 93–116.

Cox, W. R., Dixon, D. A., and Murphy, B. S. (1984). "Lateral load tests of 25.4 mm diameter piles in very soft clay in side-by-side and in-line groups." *Proc., Laterally Loaded Deep Found.: Anal. and Perf., SPT835*, ASTM, West Conshohocken, Pa.

Holloway, D. M., Moriwaki, Y., Stevens, J. B., and Perez, J. Y. (1981). "Response of a pile group to combined axial and lateral loading." *Proc., 10th Int. Conf. on Soil Mech. and Found. Engrg.*, Vol. 2, Boulimia Publishers, Stockholm, 731–734.

Huang, A. B., and Ma, M. Y. (1994). "An analytical study of cone penetration tests in granular material." *Can. Geotech. J.*, Ottawa, 31(1), 91–103.

Jamiolkowski, M., Ghionna, V. N., Lancellotta, R., and Pasqualini, E. (1988). "New correlations of penetration tests for design practice." *Proc., 1st Int. Symp. on Penetration Testing, ISOPT-1*, J. de Ruiter, ed., Balkema, Rotterdam, The Netherlands, 263–296.

Lieng, J. T. (1988). "Behavior of laterally loaded piles in sand—Large scale model tests." PhD thesis, Dept. of Civ. Engrg., Norwegian Institute of Technology, Trondheim, Norway.

Lin, S. S., and Hoe, E. (1998). "Quality control of pile foundations using NDT-case studies in Taiwan." *Transp. Res. Rec. 1633*, Transportation Research Board, Washington, D.C., 102–107.

McVay, M., Casper, R., and Shang, T. I. (1995). "Lateral response of three-row groups in loose to dense sands at 3D and 5D pile spacing." *J. Geotech. Engrg.*, ASCE, 121(5), 436–441.

Matlock, H. (1970). "Correlations for design of laterally loaded piles in soft clay." *Proc., 2nd Offshore Tech. Conf.*, Vol. 1, 577–594.

O'Neill, M. W. (1983). "Group action in offshore piles." *Proc., Spec. Conf. on Geotech. Engrg. in Offshore Pract.*, ASCE, New York, 25–63.

Reese, L. C., and Wang, S. T. (1993). *LPILE 4.0*, Ensoft, Inc., Austin, Tex.

Reese, L. C., and Wang, S. T. (1996). *GROUP 4.0 for Windows, analysis of a group of piles subjected to axial and lateral loading*. Ensoft, Inc., Austin, Tex.

Robertson, P. K., Davies, M. P., and Campanella, R. G. (1989). "Design of laterally loaded driven piles using the flat dilatometer." *ASTM Geotech. Testing J.*, 12(1), 30–38.

Wang, S. T. (1986). "Analysis of drilled shafts employed in earth-retaining structures." PhD thesis, Dept. of Civ. Engrg., University of Texas, Austin, Tex.


## NOTATION

*The following symbols are used in this paper:*

$D$ = pile diameter;
$EI$ = flexural rigidity of piles;
$E_D$ = dilatometer modulus from DMT;
$F_c$ = empirical coefficient for cohesive soils;
$F_\phi$ = empirical coefficient for cohesionless soils;
$f'_c$ = unconfined compressive strength of concrete;
$f_m$ = *p*-value reduction factor;
$f_y$ = yield stress of reinforced steel;
$G_{\max}$ = maximum shear modulus from SCPT;
$I_D$ = material index from DMT;
$J$ = empirical coefficient for cohesive soils;
$K_D$ = horizontal stress index from DMT;
$K_0$ = coefficient of earth pressure at rest;
$N$ = SPT-N value (blows/30-cm penetration);
$P_0$ = liftoff pressure from DMT;
$P_1$ = 1.1-mm expansion pressure from DMT;
$p$ = soil lateral resistance per unit length of pile;
$p_m$ = pile group *p* multiplier;
$p_{mga}$ = group pile adjustment factor from preconstruction DMT;
$p_{mgb}$ = group pile adjustment factor from postconstruction DMT;
$p_{ms}$ = single pile adjustment factor;
$p_u$ = ultimate soil lateral resistance per unit length of pile;
$q_c$ = cone tip resistance from CPT;
$s$ = pile spacing;
$u_0$ = hydrostatic pressure prior to dilatometer insertion;
$y$ = lateral deflection of pile element;
$y_c$ = lateral deflection of pile element corresponding to $p = 0.5p_u$; and
$\sigma'_v$ = effective vertical stress prior to dilatometer insertion.



J. Geotech. Geoenviron. Eng. 2001.127:385-397.